Ruoho, A., & Kyte, J. (1977) *Methods Enzymol. 46*, 523–531.
Sadasivan, E., Rothenberg, S. P., da Costa, M., & Brink, L. (1986) *Biochim. Biophys. Acta 882*, 311–321.
Schaefer, F. W., III, & Mukkada, A. J. (1976) *J. Protozool. 23*, 446–449.
Silber, R., Huennekens, F. M., & Gabrio, B. W. (1963) *Arch. Biochem. Biophys. 100*, 525–530.
Spector, R. (1977) *J. Biol. Chem. 252*, 3364–3370.
Young, J. D., Jarvis, S. M., Robins, M. J., & Paterson, A. R. P. (1983) *J. Biol. Chem. 258*, 2202–2208.
Zilberstein, D., & Dwyer, D. M. (1984) *Mol. Biochem. Parasitol. 12*, 327–336.
Zilberstein, D., & Dwyer, D. M. (1985) *Proc. Natl. Acad. Sci. U.S.A. 82*, 1716–1720.

Evidence for Functionally Distinct Glucose Transporters in Basal and Insulin-Stimulated Adipocytes†

Richard R. Whitesell,* David M. Regen, and Nada A. Abumrad
Department of Molecular Physiology and Biophysics, Vanderbilt University School of Medicine, Nashville, Tennessee 37232
Received November 16, 1988; Revised Manuscript Received May 1, 1989

ABSTRACT: The activity and K_m of glucose transport of rat adipocytes are quite variable in the basal state. This could be due to differing levels of highly saturable transport against a background of less saturable transport. Such heterogeneity could lead to differing conclusions as to the K_m of basal cells compared to insulin-stimulated cells depending on the choice of substrate, the range of concentrations tested, and the rigor of data analysis. In the present work, we used a cell preparation which was stable and partially activated by constant agitation. We used a two-component model to fit the concentration dependence of D-glucose uptake. We defined two parallel pathways of glucose entry, a high-affinity/low-capacity pathway and a low-affinity/high-capacity pathway. Both pathways were stereospecific and were inhibited by cytochalasin B. The low-affinity pathway in basal cells had 97% of the total capacity (V_{max}) with a high K_m (>50 mM). A second pathway had a very low K_m (<1 mM) and only 3% of the total capacity, but contributed to 30–60% of glucose uptake at 8 mM glucose. In insulin-stimulated cells, a pathway with a K_m of 4–5 mM dominated and contributed 85% of glucose transport. The low-affinity but not the very high affinity pathway persisted in stimulated cells, but its contribution was only 10–15% of transport at 8 mM glucose. These results suggest the presence of at least two functionally distinct transporters whose respective contributions can be characterized by nonlinear regression of data over a wide range of glucose concentrations. From the data, we conclude that an increase of the apparent affinity of glucose transport is important to insulin action and that this observation is consistent with the hypothesis that insulin recruits a functionally distinct type of transporter into the plasma membrane. These results are discussed in relation to recent immunological findings that several species of glucose transporters may coexist in the adipocyte membrane.

It has been generally accepted (Vinten & Gliemann, 1976; Olefsky, 1978; Whitesell & Gliemann, 1979) that insulin stimualtes glucose transport in adipocytes and other cells by increasing the V_{max} without altering the K_m of the process. This is consistent with the hypothesis that insulin acts primarily by mobilizing additional carriers to the plasma membrane which are functionally identical with those present in the basal state (Cushman & Wardzala, 1980; Suzuki & Kono, 1980). We have presented evidence that, under certain conditions, rat adipocytes transport glucose with a high K_m in the basal state and that this K_m can be lowered by 90% in response to environmental factors, including insulin treatment (Whitesell & Abumrad, 1985, 1986). We suggested as alternatives either that insulin activated the basal transporters or that it recruited a nonconstitutive type of glucose carrier with a higher affinity for glucose. Discriminating between these two possibilities became a significant consideration, since multiple forms of the glucose carrier have been recently identified on the basis of structural homology and immunological evidence (Kayano et al., 1988). Similar probes also identified a distinct insulin-sensitive transporter in adipocytes and muscle. This transporter was not detected in plasma membranes of resting cells which express, however, a constitutive transporter (James et al., 1987). A glucose transporter active in liver membranes transports glucose with 90% lower affinity than does the erythrocyte transporter (Axelrod & Pilch, 1983), and this may be the liver glucose transporter recently cloned by Thorens et al. (1988). These studies, which show the coexistence of more than one type of transporter in a particular tissue, would imply functional heterogeneity of transport. This heterogeneity could apply to transport K_m or substrate specificity, or both.

Okuno and Gliemann (1987), in an attempt to explain our finding that the K_m of transport was changed by insulin in the adipocyte, suggested that "basal" preparations of adipocytes may in fact be heterogeneous to varying degrees, with glucose transported simultaneously by saturable and "non-saturable" processes. They suggested that our cell preparation may have been relatively homogenous for the nonsaturable process, which is not the physiologically important pathway for glucose entry. However, they did not characterize the nonsaturable component for uptake of glucose itself as regards stereospecificity and cytochalasin B sensitivity. The choice of substrate and its inhibitability are important because of the possibility of specificity differences among the facilitative transport path-

† This work was supported by NIH Grant DK 33301 and by Grants 18665 and 181563 from the Juvenile Diabetes Foundation.
* Author to whom correspondence should be addressed.

0006-2960/89/0428-6937$01.50/0

ways. We reported evidence for such a difference in adipocytes (Whitesell & Abumrad, 1985). The V_{max} for glucose was twice as large as the V_{max} for methylglucose in basal adipocytes, while for insulin-stimulated adipocytes the difference in V_{max} for the two substrates was not significant. Significantly, two transport pathways are simultaneously active in L6 rat myoblasts, and their respective affinities for deoxyglucose and methylglucose are very different (D'Amore & Lo, 1986).

In the present work, we have examined the kinetics of stereospecific D-[^{14}C]glucose transport (corrected for L-[^{3}H]-glucose uptake) in rat adipocytes prepared as described by Okuno and Gliemann (1987) and stirred continuously as described by Toyoda et al. (1987). This resulted in a relatively stable but partially activated preparation. The basal rate was elevated to approximately 30% of the maximally stimulated rate. We characterized a highly saturable and a relatively unsaturable process as stereospecific and cytochalasin B inhibitable which were present both in basal and in stimulated cells. We assessed their respective contributions to glucose uptake over a range of concentrations.

The results are consistent with recruitment by insulin of a glucose transporter having a K_m different from that of the constitutive adipocyte transporter. The analytical procedure offers a means to evaluate the function of more than one transporter species in the plasma membrane. This could serve as an important adjunct to immunological methods which recognize a constitutive and an insulin-sensitive transporter both in the plasma membrane and in intracellular pools (James et al., 1988; Oka et al., 1988).

Materials and Methods

Considerable care was given to purification of water and to osmolarity of the solutions. Deionized water (Barnstead deionizer/charcoal filter) was distilled in such a way as to minimize volatile contaminants (collecting 80–90% of the steam by regulating the coolant flow). Glucose used was Fisher molecular biology grade and was made up into a 1 M solution and frozen. Where indicated, an isotonic solution of 300 mM glucose was used. NaCl was oven-dried, and other salts except KCl and Hepes were used in the hydrated form to ensure reproducible osmolarity. To prepare incubation medium for several experiments, concentrated stock solutions of salts were prepared, mixed, and frozen in 11.5-mL aliquots in 25-mL vials (Fisher Dilu-Vial). Each vial contained 5 mL of 1.28 M NaCl, 5 mL of 100 mM Hepes, and 0.5 mL each of 140 mM $MgSO_4$, 520 mM KCl, and 103 mM NaH_2PO_4. To prepare 50 mL of medium (medium A), the mix was thawed and rinsed into 37.2 mL of water, and 0.5 mL of 140 mM $CaCl_2$ was added. The solution was neutralized with 150 μL of 2 M NaOH. To make medium B, the same procedure was followed, but 1 g of bovine serum albumin (Sigma fraction V) was dissolved into the solution and neutralized with an additional 150 μL of 2 M NaOH.

L-[1-^{3}H]Glucose, D-[U-^{14}C]glucose, and 3-*O*-[^{3}H]methyl-D-glucose were obtained from New England Nuclear in ethanolic solution. Required portions were dried under N_2 at room temperature and redissolved in medium A just before use. $^{3}H_2O$ was obtained from the same source and made isotonic with 10 times concentrated saline before use. Cytochalasin B was obtained from Sigma and made up to 5 mM in ethanol and stored at −20 °C. Insulin was the cloned human variety from Squibb-Novo and was stored frozen as a 100 μM stock solution.

Preparation of Cells. On the morning of an experiment, the epididymal fat of one rat, killed by decapitation, was removed and rinsed in a beaker of saline prewarmed to 37 °C. Warming and all subsequent incubations were accomplished in an infant incubator. The fat pads were dripped dry and placed in a Dilu-Vial containing 4 mL of medium B and 4 μL of glucose (from a 1 M solution), 1 mg of collagenase (Worthington type III, lot 45S8973), and a 3-mm Teflon stirring magnet. This collagenase was gentler than the type used in our customary cell preparation technique, which requires type I for adequate cell yields. Digestion was for 40–60 min by stirring at a speed which was able to submerge the tissue fragments. The dispersed cells were filtered through a nylon net and washed 4 times by centrifugation in a conical tube with 8 mL of prewarmed medium B with 0.2 mM glucose, using a table-top clinical centrifuge (lowest speed setting). The cytocrit was adjusted to 40% v/v. For determination of the cytocrit, a pipet set to 8 μL was rinsed once in the cell suspension (resuspended by pipetting using a 1-mL pipet with the tip enlarged to 1 mm) and then used to fill a microhematocrit tube. The tube was sealed with clay and centrifuged 45 s at 8000*g* in a Fisher Microfuge B.

Assay of Glucose Transport. The glucose transport assay employed L-[^{3}H]glucose and D-[^{14}C]glucose as double labels. Experimental procedures were modified from earlier ones (Whitesell & Abumrad, 1985) as follows: Assay tubes were prepared with 9 μL of medium A containing glucose (from the 300 mM solution) at 3 times the final concentration and 0.5 μCi of L-[^{3}H]glucose with 0.05 μCi of D-[^{14}C]glucose. These tubes were capped and warmed in the incubator. Aliquots (500 μL) of the cell suspension were warmed 20 min with or without insulin (10 nM) and then stirred with a 3-mm Teflon magnet on a magnetic stirrer (Fisher Thermix) at 200 rpm. After 10 min of stirring, a 100-μL aliquot of cells was withdrawn and prepared for measuring medium glucose at the start of the transport assay using the hexokinase method (Bergmeyer, 1988). The transport assay was concluded within the next 3 min. For assay, a 30-μL aliquot of the stirring cells was ejected onto the 9-μL drop of substrate mixture in the assay tube, swirled vigorously by hand, and placed on a shaker (Janke Ika Vibrax) at 600 rpm. The reaction was stopped by the addition of 130 μL of ice-cold medium A containing 200 μM phloretin (stop solution) and placed on ice. Within 2 min, the cells were transferred with a 130-μL rinse into a 300-μL prechilled microfuge tube containing about 100 μL of silicone oil (Dow 200 fluid, Accumetric, Elizabethtown, KY) and about 20 μL of corn oil. The microfuge tubes were immediately centrifuged for 45 s at 8000*g*. Evidence of the adequacy of this procedure to trap intracellular radioactive glucose has been presented (Whitesell & Abumrad, 1985). The tube was cut once above the pellet and once in the silicone oil layer, and the pellet was dispersed in 1 mL of 2 mM NaOH in a scintillation vial. Five milliliters of scintillant (ACS, Amersham) was then added for double-label counting. For determination of medium radioactivity, 10 μL of the infranatant in the microfuge tube was sampled.

In each experiment, the water space in the cell pellet was measured in triplicate by addition of 30-μL aliquots of cell suspension to 9 μL of medium containing $^{3}H_2O$, the mixture being then diluted in stop solution and centrifuged and sampled like the incubations. Total water space in the pellet was calculated as $^{3}H_2O$ in the pellet (cpm) divided by concentration of $^{3}H_2O$ in the infranatant (cpm per microliter). Extracellular space measurements were made by addition of 30-μL aliquots of cell suspension to L-[^{3}H]glucose and D-[^{14}C]glucose premixed with the stop solution, followed by centrifugation and sampling. Extracellular space was calculated from this sample as L-[^{3}H]glucose in the pellet (cpm) divided by L-[^{3}H]glucose

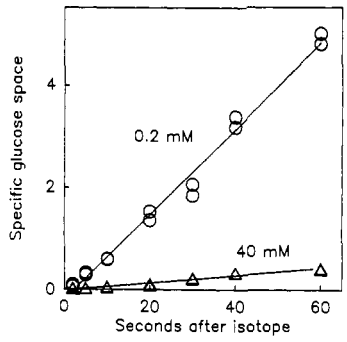

FIGURE 1: Time courses of glucose uptake in basal cells. The cells were maintained in medium B, which contained 0.1 mM glucose (measured enzymatically) at the start of the transport assay, and were sampled after addition of 0.2 mM (○) or 40 mM (△) D-glucose-containing substrate mixture (isotope). Specific D-glucose spaces were calculated as detailed under Materials and Methods (D-[^{14}C]glucose space in excess of L-[^{3}H]glucose space divided by intracellular water).

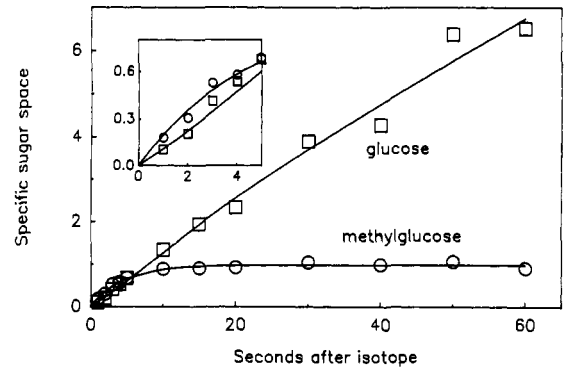

FIGURE 2: Time courses of sugar uptake in insulin-stimulated cells at low D-glucose concentration. D-[^{14}C]Glucose (0.2 mM) and [^{3}H]methylglucose (10 μM) were added as double labels, and the data are plotted as the specific sugar space. In this experiment and that of Figure 3, the L-[^{3}H]glucose space (subtracted from the total sugar space to calculate the raw specific sugar space) was measured in separate incubations. Fits by nonlinear regression were as described in the text. The insert illustrates very early sampling times.

concentration in the infranatant (cpm per microliter). Raw intracellular water space was calculated as the total water space minus the extracellular space. For the incubations, the total D-glucose space was calculated as [^{14}C]glucose in the pellet (cpm) divided by [^{14}C]glucose concentration in the medium (cpm per microliter) calculated from a representative infranatant sample. L-Glucose space (representing extracellular space plus nonspecific cellular sugar space) was calculated as L-[^{3}H]glucose in the cell pellet (cpm) divided by L-[^{3}H]-glucose concentration in the medium (cpm per microliter). Raw specific D-glucose space was calculated as total D-glucose space minus L-glucose space. Normalized specific D-glucose space was calculated as raw specific D-glucose space divided by raw intracellular water space, this being the apparent cell/medium concentration ratio. It is the concentration of D-glucose which enters stereospecifically plus metabolites of that D-glucose, divided by the concentration of D-glucose in the medium.

The rate at which the normalized specific D-glucose space rises is the specific D-glucose clearance normalized to cell water, i.e., the volume of medium containing the D-glucose entering specifically per unit time per volume of cell water. It is also cell water normalized $v/[G_0]$ and the fractional rate of equilibration. It is convenient to express this rate as microliters of medium cleared per second per milliliter of cell water, i.e., μL/(s·mL). Multiplying clearance by glucose concentration gives velocity, v. If glucose entry were unsaturable, $v/[G_0]$ would be independent of $[G_0]$, its value being the cell water normalized entry coefficient. If cell glucose entry occurred by a simple saturable process, $v/[G_0]$ would be highest (equal to V_{max}/K_m) at very low $[G_0]$ and decline toward zero with increasing $[G_0]$, $[G_0]/v$ increasing linearly with increasing $[G_0]$ (Hanes plot; Segel, 1974). If glucose entered by two processes with very different K_m's or by saturable and unsaturable processes, the Hanes plot would tend to plateau.

Nonlinear regression was performed on data, including bent Hanes plots, for which the models could not be easily transformed into linear relations. The SAS procedure NLIN was used on the specific D-glucose clearance data according to the models given in the text. Models were compared and evaluated by computing the simple correlation coefficient between observed and predicted values of the primary dependent variable (Afifi & Azen, 1979).

Results

Time Course of Stereospecific Glucose Uptake in Basal Cells. It was suggested previously (Whitesell & Abumrad, 1985) that agitation or stirring of a cell suspension might influence sugar uptake. To control for this factor in the present work, all cell suspensions were uniformly stirred before and shaken after mixing with substrates. As seen in Figure 1, uptake by basal cells was linear for 60 s at low (0.2 mM) and high (40 mM) glucose concentrations. Uptake was also linear for 60 s at intermediate concentrations (1, 3, 5, 10, and 20 mM; not shown). In basal cells, most of the cellular ^{14}C is in the form of glucose metabolites, and this is obvious at the low concentrations, where specific D-glucose space exceeded unity after 15 s. Conversion of D-glucose to metabolites served to trap intracellular ^{14}C and extend the linear phase. Eventually, some ^{14}C would be converted to escaping metabolites (pyruvate, lactate, CO_2), but the linearity of the time courses indicates that this was not significant prior to 60 s. The cold, phloretin-containing stop solution, centrifugation under corn oil, and dispersion of the cell pellet in NaOH were effective in preventing loss of metabolites after incubation. By linear regression of the time course of specific D-glucose space, initial clearance at 0.2 mM was 84 ± 3 μL/(s·mL), and that at 40 mM was 7.5 ± 0.4 μL/(s·mL). A 40-s sample appeared adequate to estimate the initial clearance at 0.2 and 40 mM.

Time Courses of Insulin-Stimulated Sugar Uptake. Similar transport tests on insulin-stimulated cells showed that estimation of the initial rate of glucose tracer uptake was feasible. Specific sugar space was measured with D-[^{14}C]glucose and [^{3}H]methylglucose present as double labels (nonspecific uptake being determined in separate samples). In these experiments, methylglucose was included as a second permeant for comparison and to document the equilibrium sugar distribution space, which was virtually the water space.

The uptake of a very low concentration of D-glucose (Figure 2) deviated slightly from the initial rate by about 15 s, as it rose above the equilibrium methylglucose space. The fit shown to the data is the two-compartment model in which the second compartment does not release isotope in the time of the experiment:

$$\text{specific sugar space} = w(1 - e^{-\lambda_t}) + kt \qquad (1)$$

In this model, w is the apparent volume of first compartment, λ_t is the fraction of steady-state level in this compartment achieved per unit time, and k is the clearance by a compartment of very slow turnover. The methylglucose time course was fit by eq 1, with w = 980 μL/mL of cell water, λ = 0.23 s^{-1}, and a negligible k [0.3 μL/(s·mL)]. Initial clearance is given by $w\lambda + k$ or 230 ± 35 μL/(s·mL). Under

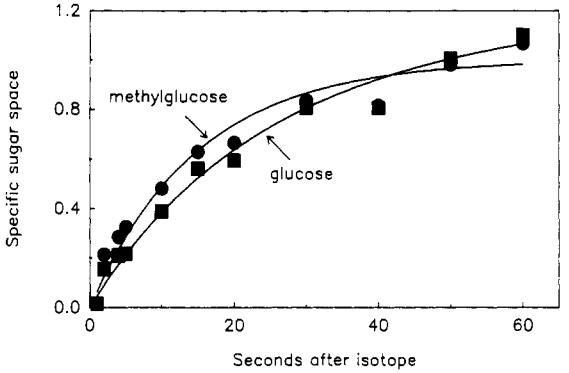

FIGURE 3: Time course of sugar uptake in insulin-stimulated cells at substantial D-glucose concentration. As for Figure 2, but glucose concentration in the assay was 20 mM.

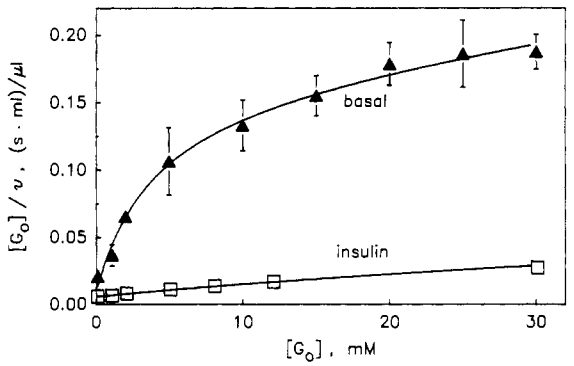

FIGURE 4: Hanes plot of glucose transport substrate dependence. The ordinate is reciprocal specific D-glucose clearance $[[G_0]/v$ in seconds milliliter per microliter], and the abscissa is substrate concentration ($[G_0]$ in millimolar). Initial rates of transport were determined as described in the legends to Figures 1 and 2 and under Materials and Methods. Each point shown represents data from five determinations. Curve fitting was by SAS NLIN, by a model with two saturable components (eq 3). The fitting coefficients are given in Table II.

the prescribed conditions, we did not witness a significant "slow phase" of methylglucose equilibration in stimulated cells after 20 s as commented on by Toyoda et al. (1987), and illustrated by Okuno and Gliemann (1987). By use of the equilibrium space from the methylglucose uptake time course fitting, the glucose data were fit to the model with $\lambda = 0.039$ s^{-1}, $k = 96$ μL/(s·mL), and $w\lambda + k = 134 \pm 13$ μL/(s·mL), and clearance was virtually linear for several seconds. Methylglucose at very low concentrations was taken up almost twice as fast as glucose in insulin-stimulated cells.

The data at 20 mM glucose (Figure 3) were fit by using the equilibrium space from the methylglucose time course in the presence of 0.2 mM D-glucose. For methylglucose, the parameter k was negligible, $\lambda = 0.063$ s^{-1}, and $w\lambda + k = 63 \pm 7$ μL/(s·mL). For glucose, eq 1 fit the data with parameters $\lambda = 0.044$ s^{-1}, $k = 2.2$ μL/(s·mL), and $w\lambda + k = 46 \pm 5$ μL/(s·mL). Stimulated glucose uptake at 20 mM was nonlinear after 20 s, but precise estimation of initial clearance could be made from samples prior to 10 s. A standard sampling time of 3 s was chosen for measuring the initial rate at a variety of glucose concentrations. In all other experiments, L-[^{3}H]glucose was present simultaneously with D-[^{14}C]glucose for precise subtraction of extracellular space and nonspecific uptake, as described under Materials and Methods. The correlation coefficient from the nonlinear regression procedure with eq 1 was greater than 0.95 in all cases.

Kinetic Heterogeneity of Glucose Transport. Figure 4 shows Hanes plots of reciprocal specific D-glucose clearance in basal and insulin-stimulated adipocytes. The Hanes plot for basal cells is very bent and tends to plateau, resolving into at least

Table I: Estimates of Parameters Describing Basal and Insulin-Stimulated Transport According to a Model with a Saturable and a Nonsaturable Component (Equation 2)[a]

	V_{max} [nmol/(s·mL)]	K_m (mM)	δ [μL/(s·mL)]	correlation coefficients
trials with basal cells				
1	33 ± 6	0.80 ± 0.13	2 ± 0.4	0.998
2	16 ± 4	0.32 ± 0.09	6 ± 1.0	0.998
3	39 ± 5	0.91 ± 0.11	4 ± 0.7	0.998
4	73 ± 7	0.70 ± 0.06	8 ± 1.3	0.999
5	64 ± 6	0.60 ± 0.06	8 ± 1.4	0.994
6	40 ± 5	0.86 ± 0.10	5 ± 0.8	0.998
7	12 ± 2	0.31 ± 0.06	6 ± 0.6	0.998
means (n = 7)	40 ± 9	0.64 ± 0.09	6 ± 0.8	
trials with insulin-treated cells				
1	330 ± 40	2.9 ± 0.32	13 ± 3	0.992
2	350 ± 100	3.4 ± 0.87	8 ± 7	0.975
3	400 ± 80	5.2 ± 0.93	7 ± 4	0.950
4	680 ± 190	4.5 ± 1.15	11 ± 8	0.974
5	1100 ± 290	7.9 ± 1.80	6 ± 8	0.978
6	350 ± 70	2.1 ± 0.38	2 ± 6	0.970
7	680 ± 140	3.4 ± 0.84	1 ± 0.3	0.979
means (n = 7)	556 ± 108	4.2 ± 0.7	7 ± 2	

[a] In basal cells, K_m refers to the nondominant, low-capacity, very high affinity component. This model ignores saturability of the dominant, low-affinity, high-capacity pathway. Correlation coefficients between observed and predicted values of the data for each trial are indicated. Parameters from each trial are given with the asymptotic standard errors of the SAS NLIN procedure. Means are given with standard errors calculated from individual parameter values.

two pathways of very different characteristics. A similar bend in the Hanes plot from insulin-stimulated cells is evident but not as pronounced. We examined the adequacy of two models in accounting for these data. One model consisted of a pathway exhibiting Michaelis–Menten kinetics with a parallel nonsaturable pathway:

$$v/[G_0] = (V/K)/(1 + [G_0]/K) + \delta \quad (2)$$

where V is V_{max} in nanomoles per second per milliliter, K is K_m in millimolar, and δ is a clearance constant in microliters per second per milliliter. The other model consisted of two parallel pathways exhibiting Michaelis–Menten kinetics:

$$v/[G_0] = (V_1/K_1)/(1 + [G_0]/K_1) + (V_2/K_2)/(1 + [G_0]/K_2) \quad (3)$$

where subscripts 1 and 2 identify the two pathways.

We found that the simpler model, eq 2, was adequate in the sense that correlation coefficients were very high (Table I). According to this model, the saturable pathway of basal cells had a very high affinity, $K_m = 0.6$ mM, and a low capacity, $V_{max} = 39$ nmol/(s·mL), such that the unsaturable pathway was more important that the saturable pathway at sugar concentrations exceeding about 3 mM. According to this model, insulin increased the K_m of the saturable pathway 6-fold (to 4 mM) and increased its capacity 14-fold, without significantly affecting the unsaturable pathway. This might reflect recruitment to the membrane of a distinct carrier of intermediate affinity, completely obscuring the very high affinity pathway and almost obscuring the low-affinity pathway (resulting in larger variance of δ). Alternatively or additionally, some of the transporters in basal cells might have changed affinity and/or activity with insulin treatment and contributed to the intermediate affinity uptake.

The more complex model, eq 3, having a fourth parameter, fit certain experiments and failed to converge with data from other experiments. The lines through the data of Figure 4

Table II: Coefficients Describing Transport According to a Model with Two Saturable Transport Components (Equation 3)

	pathway	V_{max} [nmol/(s·mL)]	K_m (mM)	correlation coefficient	% contribution at 8 mM
basal cells	1	22	0.24	0.96	34
	2	870	140		66
insulin-treated cells	1	780	4.9	0.95	81
	2	2400	169		19

Table III: Comparison between Low-Affinity Clearance of D-Glucose, Total Residual Clearance in the Presence of Cytochalasin B, and L-Glucose Clearance[a]

	clearance [μL/(s·mL)]	
	basal	insulin
low-affinity component	4.6 ± 1.9	16 ± 6
total D-glucose clearance with cytochalasin B (μM)		
0	123 ± 13	237 ± 50
20	1.6 ± 0.3	5.4 ± 0.6
60	1.3 ± 0.2	3.3 ± 0.5
100	0.8 ± 0.08	2.9 ± 0.2
total L-glucose clearance with cytochalasin B (μM)		
0	0.30 ± 0.03	0.25 ± 0.03
20	0.15 ± 0.06	0.11 ± 0.03
60	0.15 ± 0.10	0.14 ± 0.02
100	0.08 ± 0.01	0.18 ± 0.01

[a] The low-affinity component of specific D-glucose clearance from control and inhibited incubations was determined by fitting to eq 2. Where indicated, cytochalasin B from a 5 mM stock solution in ethanol was added simultaneously with substrate mixture, while controls and inhibited incubations contained a constant amount of ethanol.

show the fitting of the aggregate data from several experiments by eq 3, the parameters being given in Table II. This treatment agreed with the simpler one, showing a very high affinity pathway (K_m = 0.24 mM) of low capacity [V_{max} = 22 nmol/(s·mL)] in basal cells, together with a pathway of very low affinity more roughly characterized, having a high K_m and V_{max} [140 mM and 870 nmol/(s·mL), respectively]. According to this model, again, insulin increased the K_m of the first component (to 4.9 mM) and increased the capacity of both pathways [to 780 and 2400 nmol/(s·mL)]. The K_m of the second pathway was not affected significantly by insulin (169 vs 140 mM).

Stereospecificity and Cytochalasin B Inhibitability. Since eq 2 (with a nonsaturable pathway paralleling a saturable pathway) fit the data adequately, and since eq 3 (with two saturable pathways) fit the data with a low-affinity pathway which was not appreciably saturated by our highest glucose concentration, the kinetic data do not establish whether the low-affinity pathway was mediated transport or simple diffusion. Evidence of cytochalasin B inhibitability and stereospecificity is more conclusive, however. L-Glucose clearance was negligible compared to either pathway [0.3 μL/(s·mL) at most, Table III]. Thus, total D-glucose uptake (without correction for L-glucose uptake) was always at least 99% specific. This was perhaps partly due to the method of assay, which involved a dilution in stop solution. The contents of any "leaky" cells, including L- and D-glucose, could thus be diluted out. The important role of L-glucose was to provide a sample-by-sample subtraction of extracellular contamination, in addition to correcting for a very small component of nonspecific uptake. The total specific D-glucose clearance in the presence of 100 μM cytochalasin B (including high- and low-affinity components) was less than 20% of the uninhibited low-affinity component of D-glucose uptake. The stereospecific transport which was uninhibitable may be inhibited at very high doses of cytochalasin B, or may be taken up by an insensitive pathway. The data do not distinguish between these possibilities. Characterization of the low-affinity transport component as stereospecific and cytochalasin B sensitive supports the kinetic evidence that it is carrier-mediated and saturable.

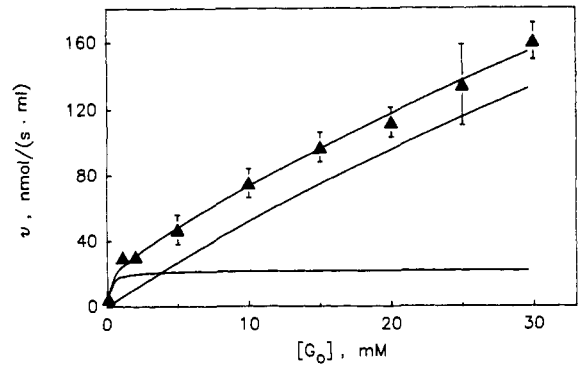

FIGURE 5: Contributions of low- and high-affinity components to the transport of varied glucose concentrations in basal cells. The calculated curves for the low- and high-K_m components were generated as described in the text from the fitting coefficients given in Table II.

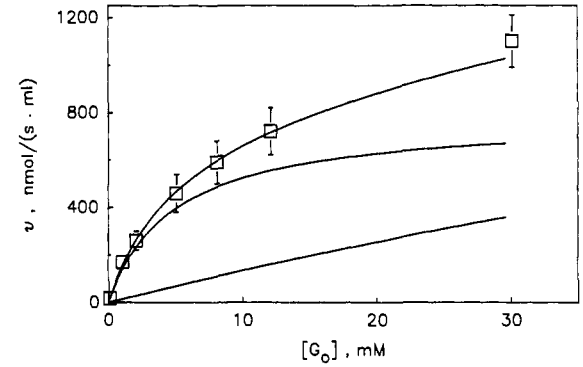

FIGURE 6: Contributions of low- and high-affinity components to the transport of varied glucose concentrations in insulin-stimulated cells. As for Figure 5, but for insulin-stimulated cells.

Contributions of High- and Low-Affinity Glucose Transport Pathways to Total Glucose Uptake. As mentioned, clearance is uptake rate relative to external concentration, the reciprocal of which is plotted against external concentration in Figure 4, as a Hanes plot. The two terms of eq 3 are the clearances contributed by the two pathways of differing saturability. Clearance multiplied by external concentration yields uptake rate, v, in nanomoles per second per milliliter.

Figure 5 shows specific D-glucose uptake rates (data points) observed in basal cells plotted against external glucose concentration. Uptake increased almost linearly with increasing external glucose concentration up to the highest concentration tested (30 mM). The upper curve shows total uptake rates predicted by eq 3 with the parameters of Table II. In this form, one can see intuitively that glucose entered by at least two pathways of very different affinities and that the data are adequately accounted for by a two-component model. The contributions of these two pathways at various concentrations are shown in the lower two lines. The low-affinity pathway dominated at concentrations above 3 mM, accounting for the unsaturability of total uptake. At 8 mM, the low-affinity pathway contributed 66% of total uptake.

For insulin-stimulated cells (Figure 6), the picture was quite different. In this case, transport was moderately saturable in the physiological range. A low-affinity component was significant as in the basal preparation, but it was no longer dominant in the physiological range of glucose concentrations.

In contrast, a medium-affinity pathway catalyzed the major fraction of uptake in these cells at all concentrations shown. The average contribution of the low-affinity pathway at 8 mM was 10% ± 2% for stimulated cells.

Discussion

Two parallel mechanisms of glucose entry appear to exist in basal cells under the conditions specified. Our data show a low-affinity/high-capacity pathway which is dominant and which we had documented earlier. In addition, we found a very high affinity/low-capacity pathway. Both mechanisms are stereospecific for glucose and sensitive to cytochalasin B. The low-affinity pathway contributed approximately 60% to the total glucose transport in basal cells at 8 mM and became more dominant as the glucose concentration increased. When the data were analyzed in terms of two saturable pathways (Table III), insulin caused an increase in the V_{max} of the low-affinity pathway. Due to its lack of dominance in insulin-stimulated cells, the characterization of the low-affinity pathway was somewhat tentative, however. The major effect of insulin was to introduce a transport pathway with an intermediate K_m of 4–5 mM. James et al. (1988) present immunological evidence that insulin recruits two types of carriers, one which is peculiar to insulin-stimulable tissues and a proportion of carriers of the same type as are already expressed in the plasma membrane of basal cells. Thus, both the kinetic evidence and the immunological evidence are consistent with the hypothesis that insulin brought about a translocation of medium- and possibly low-affinity carriers to the plasma membrane, which contains a constitutive low-affinity carrier. The present experiments do not rule out conversion of low-affinity or very high affinity transporters to medium-affinity ones. Some treatments, including substrate deprivation and stirring, appeared to increase the affinity of transport without significantly changing the capacity (Whitesell & Abumrad, 1986). The minor, very high affinity carrier which we observe may be a carrier whose kinetic characteristics vary tremendously in response to environmental factors. In fact, the collagenase or method of cell preparation or the constant stirring of the cell suspension may have been responsible for the presence of the very high affinity pathway which we did not observe previously in basal cells (Whitesell & Abumrad, 1985).

We believe that several factors, including data analysis, substrate specificity, and cell preparation, have played a role in the detection of transport components with various K_m's in adipocytes. The K_m and V_{max} that one would obtain from data collected by using a limited range of glucose concentrations would depend on the concentration range and the mixture of transporters present in the cells. For data from basal cells containing a modest admixture of high-affinity or medium-affinity transporters, a simple linear regression of Hanes plots over the 4–20 mM range will underestimate both the K_m of the low-affinity component and the V_{max} of the combined transporters. Thus, characterization of glucose transport might often require a wide range of glucose concentrations, a two-component model, and nonlinear regression. Recently, D'Amore and Lo (1986) demonstrated the presence of two transport systems in L-6 myoblasts, one of which was specific for deoxyglucose and one which was specific for methylglucose. Therefore, analogue studies in general may be subject to special pitfalls. Using the native substrate is also an important consideration since we[1] see no effect of insulin on the K_m for deoxyglucose uptake. Also, we and others[2] see no indication of heterogeneity in basal cells when using methylglucose as substrate. The differences among glucose, deoxyglucose and methylglucose appear to relate to their interaction with the glucose carriers and not to metabolic interactions. This surmise is based on the observation that preincubation with glucose before measurement of tracer flux did not affect the interpretation of coexisting low- and high-K_m components.[1]

Taken together, these observations justify a reexamination of transport kinetics in many systems, with the aim to describe the kinetics of the uptake of the native substrate, glucose, with the appropriate models and statistical tools outlined in this paper. We suggest from work by us and others that effects on the apparent transport K_m for glucose may be widely significant, for example, in the glucose metabolism of rat red blood cells (Abumrad et al., 1988), thymocytes (Whitesell & Regen, 1978), and muscle (Ploug et al., 1987), as well as in the adipocyte (Whitesell & Abumrad, 1985). In addition, the transporter heterogeneity of the adipocyte, identified by immunological evidence (Pilch et al., 1988; Oka et al., 1988) and in the present work by kinetic evidence, may prove to be a general case. The techniques described here can be adapted to tissue culture systems, where they would provide a direct functional assay for multiple transporter function in cells showing immunological reactivities for more than one transporter species.

Acknowledgments

Assistance in running and interpreting SAS NLIN was generously provided by Steven Torres, Vanderbilt Computer Center, User Services Division. The technical assistance of Diana K. Pelletier is gratefully acknowledged.

References

Abumrad, N. A., Briscoe, P., Beth, A. H., & Whitesell, R. R. (1988) *Biochim. Biophys. Acta 938*, 222–230.

Afifi, A. A., & Azen, S. P. (1979) in *Statistical Analysis: A computer oriented approach*, 2nd ed., Academic Press, New York.

Axelrod, J. D., & Pilch, P. F. (1983) *Biochemistry 22*, 2222–2227.

Bergmeyer, H. U. (1988) *Methods of Enzymatic Analysis*, VCH Verlagsgesellschaft, Weinheim, FDR.

Cushman, S., & Wardzala, L. (1980) *J. Biol. Chem. 255*, 4758–4762.

D'Amore, T., & Lo, T. C. Y. (1986) *J. Cell. Physiol. 127*, 95–105.

James, D. E., Brown, R., Navarro, J., & Pilch, P. F. (1988) *Nature 333*, 183–185.

Kayano, T., Fukumoto, H., Eddy, R. L., Fan, Y., Byers, M. G., Shows, T. B., & Bell, G. I. (1988) *J. Biol. Chem. 263*, 15245–15248.

Oka, Y., Asano, T., Shibasaki, Y., Kasuga, M., Kanazawa, Y., & Takaku, F. (1988) *J. Biol. Chem. 263*, 13432–13439.

Okuno, Y., & Gliemann, J. (1987) *Diabetologia 30*, 426–430.

Olefsky, J. M. (1978) *Biochem. J. 172*, 137–145.

Ploug, T., Galbo, H., Vinten, J., Jorgensen, M., & Richter, E. (1987) *Am. J. Physiol. 253*, E12–20.

Segel, I. H. (1975) *Enzyme Kinetics*, Wiley, New York.

Suzuki, K., & Kono, T. (1980) *Proc. Natl. Acad. Sci. U.S.A. 77*, 2542–2545.

Thorens, B., Sarkar, H. K., Kaback, H. R., & Lodish, H. F. (1988) *Cell 55*, 281–290.

[1] R. R. Whitesell and N. A. Abumrad, unpublished observations.

[2] T. Kono and N. Toyoda, personal communication.

Toyoda, N., Flanagan, J., & Kono, T. (1987) *J. Biol. Chem. 262*, 2737–2745.
Vinten, J., & Gliemann, J. (1976) *J. Biol. Chem. 251*, 794–800.
Whitesell, R. R., & Regen, D. M. (1978) *J. Biol. Chem. 253*, 7289–7294.
Whitesell, R. R., & Gliemann, J. (1979) *J. Biol. Chem. 254*, 5276–5283.
Whitesell, R. R., & Abumrad, N. A. (1985) *J. Biol. Chem. 260*, 2894–2899.
Whitesell, R. R., & Abumrad, N. A. (1986) *J. Biol. Chem. 261*, 15090–15096.

A Photoactivable Phospholipid Analogue That Specifically Labels Membrane Cytoskeletal Proteins of Intact Erythrocytes†

Deepti Pradhan,‡ Patrick Williamson,§ and Robert A. Schlegel*,‡,‖
Department of Molecular and Cell Biology, The Pennsylvania State University, University Park, Pennsylvania 16802, and Department of Biology, Amherst College, Amherst, Massachusetts 01002
Received January 20, 1989; Revised Manuscript Received April 18, 1989

ABSTRACT: A radioactive photoactivable analogue of phosphatidylethanolamine, 2-(2-azido-4-nitrobenzoyl)-1-acyl-*sn*-glycero-3-phospho[^{14}C]ethanolamine ([^{14}C]AzPE), was synthesized. Upon incubation with erythrocytes in the dark, about 90% of [^{14}C]AzPE spontaneously incorporated into the cells; of this fraction, about 90% associated with the membrane, all of it noncovalently. Upon photoactivation, 3–4% of the membrane-associated probe was incorporated into protein. Analysis of this fraction by sodium dodecyl sulfate–polyacrylamide gel electrophoresis, as well as extraction of labeled membranes with alkali or detergent, showed that the probe preferentially labeled cytoskeletal proteins. [^{14}C]AzPE appears to be a useful tool for the study of lipid–protein interactions at the cytoplasmic face of the plasma membrane of intact cells.

Molecular analysis of cell structure is heavily dependent on the use of probes which interact with cells in a specific, predictable manner; the site of interaction of probes on or within the cell, monitored by using radioactivity, fluorescence, absorption, electron spin resonance, or other detectable signals, provides information on the molecular constitution and topography of the cell. Photoactivable probes offer the unique advantage that they remain inert until they reach their targeted site, thus reducing nonspecific labeling. In studies of cell membranes, hydrophobic probes of this sort have been used to identify hydrophobic regions of membrane proteins (Bayley & Knowles, 1980; Brunner, 1981; Pradhan & Lala, 1987), and hydrophilic probes have been used to label surface proteins (Staros et al., 1974; Dockter, 1979). Although photoactivable phospholipid analogues have been synthesized for use as amphipathic probes (Bisson et al., 1979; Ross et al., 1982; Burnett et al., 1985), they have been used chiefly to study the interactions of integral membrane proteins with phospholipids; none have been applied to peripheral membrane proteins, which lie in proximity to the membrane. A variety of investigations would profit from the availability of a photoactivable phospholipid probe which could specifically label and thus identify proteins lining the cytoplasmic side of the plasma membrane of intact cells.

The human erythrocyte provides a simple cell in which to test the efficacy of such a probe. In particular, the known arrangement of phospholipids in the erythrocyte membrane facilitates the design of a probe with the desired specificity. Phosphatidylcholine (PC)[1] and sphingomyelin reside chiefly in the outer leaflet of the erythrocyte plasma membrane, whereas phosphatidylethanolamine (PE) is more abundant in and phosphatidylserine (PS) is restricted to the inner leaflet of the bilayer (Bretscher, 1973; Op den Kamp, 1979). Targeting a phospholipid-based probe to the internal surface of the plasma membrane, therefore, requires that the photoactivable phospholipid have either an ethanolamine or a serine as the headgroup.

The probe must also possess several other important characteristics. First, it should spontaneously partition into the plasma membrane from the aqueous medium. Since attachment of an aromatic moiety directly to the C2 position of the glycerol backbone facilitates transfer of phospholipids into cells (Bisson & Montecucco, 1985), attachment of an aromatic photoactivable group at this point should enhance uptake. Second, once inserted into the plasma membrane, the probe should migrate to its cytoplasmic side. If the photoactivable group is small, the analogue will resemble a lysophospholipid, which is translocated across the bilayer more readily than the parent phospholipid (Bergmann et al., 1984). In addition, the erythrocyte membrane is equipped with an activity which transports aminophospholipids from the outside to the inside of the membrane (Seigneuret & Devaux, 1984; Zachowski et al., 1986). If this activity applies to a PE-derived probe, net inward movement of the molecule would be favored. Third, if the proteins in apposition to the inner surface of the membrane are to be labeled, the photoactivable moiety should be

† This work was supported by the U.S. Public Health Service (CA28921).
‡ The Pennsylvania State University.
§ Amherst College.
‖ Established Investigator of the American Heart Association.

[1] Abbreviations: AzBA, 2-azido-4-nitrobenzoic acid; AzPC, 2-(2-azido-4-nitrobenzoyl)-1-acyl-*sn*-glycero-3-phosphocholine; [^{14}C]AzPE, 2-(2-azido-4-nitrobenzoyl)-1-acyl-*sn*-glycero-3-phospho[^{14}C]ethanolamine; GSH, reduced glutathione; HPLC, high-performance liquid chromatography; PC, phosphatidylcholine; PE, phosphatidylethanolamine; PS, phosphatidylserine; SDS–PAGE, sodium dodecyl sulfate–polyacrylamide gel electrophoresis; TCA, trichloroacetic acid; TLC, thin-layer chromatography.

0006-2960/89/0428-6943$01.50/0